Electrodeposited, "Textured" Poly(3-hexyl-thiophene) (e-P3HT) Films for Photovoltaic Applications

Erin L. Ratcliff, Judith L. Jenkins, Ken Nebesny, and Neal R. Armstrong*

Department of Chemistry, University of Arizona, Tucson, Arizona 85721

Received March 19, 2008. Revised Manuscript Received June 7, 2008

Organic photovoltaic devices have been created on activated and modified ITO electrodes from electrodeposited poly(3-hexylthiophene) (e-P3HT) donor layers, using pulsed-potential-step (PPS) electrodeposition protocols. PPS electrodeposition uses a series of potential steps of diffusion-controlled e-P3HT deposition, alternated with rest periods where no deposition occurs and the diffusion layer region near the electrode/solution interface refills with thiophene monomer. To create the most photoactive e-P3HT films, a "carpet" layer of polymer was first deposited using dual step chronoamperometry, to create a smooth, pinhole-free film on the ITO electrode. PPS electrodeposition was subsequently used to electrodeposit additional polymer and texture the e-P3HT surface, as revealed by both AFM and SEM. The extent of doping of the polymer film was controlled by the last applied rest potential and monitored by anion incorporation into the e-P3HT film using X-ray photoelectron spectroscopy (XPS). Textured and electrochemically doped e-P3HT films were used as the donor layer in photovoltaic devices, using vacuum deposited C_{60} as the electron acceptor/electron transport layer: (ITO/e-P3HT/C_{60}/BCP/Al). The performance of these ultrathin OPVs was markedly dependent upon the degree of electrochemical doping of the P3HT layers. The best OPV performance was obtained for e-P3HT films with an average doping level (ratio of oxidized to reduced thiophene units) of approximately 35%, as estimated by XPS. At 100 mW/cm^2 white light illumination, optimized devices give a $V_{OC} \sim 0.5$ V and a maximum $J_{SC} \sim 3$ mA/cm^2, with series resistance (R_S) below 1 $\Omega \cdot$cm^2, shunt resistance (R_P) in excess of 160 k$\Omega \cdot$cm^2, fill-factors (FF) of approximately 0.65, and an overall power conversion efficiency of approximately 1%. These results demonstrate the promise of electrochemical protocols for the creation of a variety of hybrid energy conversion materials.

Introduction

A number of recent organic photovoltaic devices (OPVs) with poly(thiophene) donor/hole transport layers have been created from spin-cast films, often blended with electron transport layers, such as 1-(3-methoxycarbonyl)propyl-1-phenyl-[6,6]-methanofullerene (PCBM).[1−6] Recent improvements of OPV device efficiency have focused on the creation of an interpenetrating, phase separated donor−acceptor network in a mixed heterojunction,[4,6−8] with overall increased surface area of the donor−acceptor interface.[1−3] An ideal architecture would consist of interdigitated columns with dimensions of the light absorbing phases on the order of the exciton diffusion length, ensuring high probability of charge dissociation, while maintaining low resistance for charge transport.[3−6,9] Theoretical calculations predict such morphologies could increase the overall external quantum efficiencies (EQEs) by a factor of 2 over randomly oriented spin cast blends.[6,10] Possible avenues to fabricate interdigitated columns include vacuum deposition,[9] nanolithography (i.e., microcontact printing), track-etched surfaces as templates,[11−14] and electrochemical methods (templateless synthesis, template-assisted synthesis, and molecular template assisted synthesis).[15] The best P3HT/PCBM device performance to date has been achieved with careful spin casting and annealing of donor/acceptor spin cast films;[7,16−21] however, it is clear that any charge carriers generated in regions of the thin film isolated from the charge collecting

* To whom correspondence should be addressed. E-mail: nra@u.arizona.edu.

(1) Yu, G.; Gao, J.; Hummelen, J. C.; Wudl, F.; Heeger, A. J. *Science* **1995**, *270*, 1789–1791.
(2) Halls, J. J. M.; Walsh, C. A.; Greenham, N. C.; Marseglia, E. A.; Friend, R. H.; Moratti, S. C.; Holmes, A. B. *Nature* **1995**, *376*, 498–500.
(3) Gunes, S.; Neugebauer, H.; Sariciftci, N. S. *Chem. Rev.* **2007**, *107*, 1324–1338.
(4) Blom, P. W. M.; Mihailetchi, V. D.; Koster, L. J. A.; Markov, D. E. *Adv. Mater.* **2007**, *19*, 1551–1566.
(5) Koster, L. J. A.; Mihailetchi, V. D.; Blom, P. W. M. *Appl. Phys. Lett.* **2006**, 88.
(6) Marsh, R. A.; Groves, C.; Greenham, N. C. *J. Appl. Phys.* **2007**, 101.
(7) Campoy-Quiles, M.; Ferenczi, T.; Agostinelli, T.; Etchegoin, P. G.; Kim, Y.; Anthopoulos, T. D.; Stavrinou, P. N.; Bradley, D. D. C.; Nelson, J. *Nat. Mater.* **2008**, *7*, 158–164.
(8) Boucle, J.; Ravirajan, P.; Nelson, J. *J. Mater. Chem.* **2007**, *17*, 3141–3153.
(9) Hiramoto, M.; Yamaga, T.; Danno, M.; Suemori, K.; Matsumura, Y.; Yokoyama, M. *Appl. Phys. Lett.* **2006**, 88.
(10) Peumans, P.; Forrest, S. R. *Appl. Phys. Lett.* **2001**, *79*, 126–128.
(11) Mazur, M.; Tagowska, M.; Palys, B.; Jackowska, K. *Electrochem. Commun.* **2003**, *5*, 403–407.
(12) Pra, L. D. D.; Ferain, E.; Legras, R.; Demoustier-Champagne, S. *Nucl. Instrum. Methods Phys. Res., Sect. B* **2002**, *196*, 81–88.
(13) Demoustier-Champagne, S.; Stavaux, P. Y. *Chem. Mater.* **1999**, *11*, 829–834.
(14) Demoustier-Champagne, S.; Ferain, E.; Jerome, C.; Jerome, R.; Legras, R. *Eur. Polym. J.* **1998**, *34*, 1767–1774.
(15) Malinauskas, A.; Malinauskiene, J.; Ramanavicius, A. *Nanotechnology* **2005**, *16*, R51−R62.
(16) Li, G.; Shrotriya, V.; Huang, J. S.; Yao, Y.; Moriarty, T.; Emery, K.; Yang, Y. *Nat. Mater.* **2005**, *4*, 864–868.
(17) Yang, C. Y.; Hu, J. G.; Heeger, A. J. *J. Am. Chem. Soc.* **2006**, *128*, 12007–12013.

10.1021/cm8008122 CCC: $40.75
Published on Web 08/28/2008

(top or bottom) electrodes will suffer trapping and recombination, resulting in photocurrent loss.[6] Even in ideally networked blended heterojunction materials, the low dielectric constant of the organic films limits the probability of exciton dissociation (dissociation of geminate electron/hole pairs),[4,6] leading to a significant field-dependence of the photocurrent and low fill-factors in the OPV.

Electrodeposition is well-known as a means of fabricating thin films of conducting polymers, such as poly(thiophenes). Key advantages stem from combining polymer synthesis and film formation into a single step, limiting the need for oxidants to initiate polymerization. The polymer films can be "wired" to the electrode surface, decreasing contact resistance without the need for additional layers, such as the traditional PEDOT:PSS, and permitting homogeneous film coverage over nonplanar substrates. Manipulation of electrochemical parameters, such as applied potential, can control oxidation states, yielding variable electronic conductivities and/or optical properties, while also controlling the local concentrations of coincorporated electrolytes at the polymer solution interface, influencing the local dielectric constant at the electrode/polymer interface. Moreover, it is well-known that morphological control can be achieved through the employment of template or lithography technologies. Conducting polymer colloids can also be prepared by the optimization of electropolymerization parameters such as monomer concentration, polymerization time, and working electrode morphology.[15,22−24]

Previous electrochemical methods for active layer formation in photovoltaic cells have primarily focused on film growth using cyclic voltammetry because of its convenience and because it provides information about oxidative doping during the deposition process. It is difficult, however, to resolve the potential and time effects on polymer deposition from one another using CV methods,[25] and it is difficult to control the rate of film growth and film thickness. As a film like P3HT is doped from the neutral state to the conductive oxidized state, electrolyte species are drawn in or out of the film to maintain charge neutrality.[25,26] While doping may be controlled electrochemically, successive cycling (i.e., cyclic voltammetric growth) may result in localized film degradation.[27−29] Photovoltaic devices created from single-layer electrodeposited poly(3-methylthiophene) (PMeT) or poly(thiophene) (PT) films (deposited galvanostatically) have been recently reported (ITO/PMeT or PT/Al), with high open-circuit photovoltages (V_{OC} = ca. 1 V). The thickness of these electrodeposited layers, however, usually exceeded the exciton diffusion length in poly(thiophenes) by at least 10× and photocurrents of only 0.01−0.1 mA/cm^2, low fill factors, and low overall power conversion efficiencies were observed.[30−32] Ultimately, the issues with current OPVs from electrodeposited films arise from well understood problems with single layer OPVs: exciton dissociation may occur near one of the contacting electrodes, and exciton quenching and uncontrolled recombination events may significantly lower power conversion efficiencies.[4,6,33−35]

The work presented here focuses on the formation of thin, electrochemically deposited P3HT (e-P3HT) films, optimally doped to contain both the photoactive, neutral form and the electronically conductive, doped form of P3HT, chosen specifically to improve photovoltaic device performance. We demonstrate here the utilization of pulsed-potential-step (PPS) protocols as an alternative method for poly(3-hexylthiophene) (e-P3HT) electrodeposition, controlling both the morphology and the internal doping of the resultant e-P3HT films. This approach to P3HT deposition provides an optimally doped film with controllable roughening of the near-surface region.

Photoactive heterojunctions have been subsequently formed with vacuum deposited C_{60} and bathocuproine (BCP) to give a cell with the configuration ITO/e-P3HT/C_{60}/BCP/Al. We intentionally chose to make cells similar to vacuum deposited planar heterojunction platforms, the only difference being the use of the e-P3HT layer as the donor material.[33−36] While this approach does not take full advantage of the interdigitation of donor and acceptor phases that the PPS protocol provides, it leads to an OPV with statistically significant reproducibility in performance, the only variable being the way in which the e-P3HT film is produced and doped. Optimally doped versions of these devices show only a small field dependence of the photocurrent at potentials negative of the open-circuit voltage (V_{OC}), with modest power conversion efficiencies but high fill factors and low series resistance (R_S). These device parameters are tunable depending upon the electrochemical doping of the e-P3HT layers, and the optimum PV response is obtained from e-P3HT layers which are doped to contain approximately 35% oxidized thiophene units within the film. Electrodeposited layers such as these will form the basis for future PV cells based on polymer/electron acceptor blends and polymer/semiconductor nanoparticle or oxide nanoparticle blends, where the nanoparticle is electrochemically captured into the polymer host via capping ligands which are terminated in

(18) Kim, K.; Liu, J.; Namboothiry, M. A. G.; Carroll, D. L. *Appl. Phys. Lett.* **2007**, *90*.
(19) Ma, W. L.; Yang, C. Y.; Gong, X.; Lee, K.; Heeger, A. J. *Adv. Funct. Mater.* **2005**, *15*, 1617–1622.
(20) Reyes-Reyes, M.; Kim, K.; Carroll, D. L. *Appl. Phys. Lett.* **2005**, 87.
(21) Padinger, F.; Rittberger, R. S.; Sariciftci, N. S. *Adv. Funct. Mater.* **2003**, *13*, 85–88.
(22) Aboutanos, V.; Barisci, J. N.; Innis, P. C.; Wallace, G. G. *Colloids Surf., A* **1998**, *137*, 295–300.
(23) Schuhmann, W.; Kranz, C.; Wohlschlager, H.; Strohmeier, J. *Biosens. Bioelectron.* **1997**, *12*, 1157–1167.
(24) Kiani, M. S.; Mitchell, G. R. *Synth. Met.* **1992**, *48*, 203–218.
(25) Hillman, A. R.; Mallen, E. F. *J. Electroanal. Chem.* **1987**, *220*, 351–367.
(26) Li, F. B.; Albery, W. J. *J. Chem. Soc., Faraday Trans.* **1991**, *87*, 2949–2954.
(27) Ocon, P.; Herrasti, P.; Rojas, S. *Polymer* **2001**, *42*, 2439–2448.
(28) Otero, T. F.; Angulo, E.; Santamaria, C.; Rodriquez, J. *Synth. Met.* **1993**, *54*, 217–222.
(29) Tsai, E. W.; Basak, S.; Ruiz, J. P.; Reynolds, J. R.; Rajeshwar, K. *J. Electrochem. Soc.* **1989**, *136*, 3683–3689.
(30) Valaski, R.; Canestraro, C. D.; Micaroni, L.; Mello, R. M. Q.; Roman, L. S. *Sol. Energy Mater. Sol. Cells* **2007**, *91*, 684–688.
(31) Valaski, R.; Lessmann, R.; Roman, L. S.; Hummelgen, I. A.; Mello, R. M. Q.; Micaroni, L. *Electrochem. Commun.* **2004**, *6*, 357–360.
(32) Takahashi, K.; Tsuji, K.; Imoto, K.; Yamaguchi, T.; Komura, T.; Murata, K. *Synth. Met.* **2002**, *130*, 177–183.
(33) Forrest, S. R. *MRS Bull.* **2005**, *30*, 28–32.
(34) Rand, B. P.; Burk, D. P.; Forrest, S. R. *Phys. Rev. B* **2007**, 75.
(35) Tang, C. W. *Appl. Phys. Lett.* **1986**, *48*, 183–185.
(36) Brumbach, M.; Placencia, D.; Armstrong, N. R. *J. Phys. Chem. C* **2008**, *112*, 3142–3151.

alkyl-thiophenes or more electron-rich ethylenedioxy thiophenes (PEDOT or ProDOT).[37]

Experimental Section

Chemicals. 3-Hexylthiophene (3-HT), 3-thiophene acetic acid (3-TAA), and tetrabutylammonium hexafluorophosphate (TBAHFP) were used as purchased (Aldrich). Fullerene (C_{60}) was purchased from MerCorp (Tucson, AZ), and bathocuproine (BCP) was obtained from Aldrich; both were purified by triple sublimation before use. Aluminum for top contacts was purchased from Alpha Aesar.

Substrate Preparation. Indium tin oxide (ITO) on glass was purchased from Colorado Concept Coating, LLC, with a sheet resistance of ~15 Ω/□ and a film thickness of ~100 nm. The ITO was cut into 1 in. squares and cleaned in detergent (diluted Triton X-100) followed by successive sonication in 50:50 ethanol/DI water and pure ethanol. Slides were then briefly etched using a 57% HI/water solution (Aldrich) as discussed recently.[38,39] ITO electrodes were exposed to the acid solution for approximately 10 s, followed by rinsing with Millipore water while using a spin coater (Integrated Technologies Inc.) at 4000 rpm. These acid-activated ITO slides were then immediately soaked in ~10 mM solutions of 3-TAA in acetonitrile for at least 30 min, rinsed with acetonitrile, and dried under a stream of nitrogen.

Electrochemistry. e-P3HT films were electrochemically deposited using a series of potential steps with a CH1030A potentiostat (CH Instruments, Inc., Austin, TX). A standard three electrode setup was used (electroactive area = 0.76 cm^2), with the activated, 3-TAA-modified ITO working electrode directly across from a counter electrode, which was generally a second piece of ITO, versus a Ag^+ (0.01 M $AgNO_3$, 0.1 M TBAHFP, CH_3CN)/Ag reference electrode (Bioanalytical Systems). An initial "carpet layer" of P3HT was deposited by stepping the ITO potential to +1.4 V for 0.5 s, followed by stepping back to +1.35 V for 10−25 s, in a 10 mM solution of 3-hexylthiophene in 0.1 M TBAHFP in acetonitrile. Texturing these carpet-layer e-P3HT films was accomplished by additional PPS protocols which are described in detail in the text (10 mM 3-hexylthiophene in 0.1 M TBAHFP/acetonitrile).

OPV Fabrication and Characterization. After electrodeposition, the e-P3HT/ITO films were immediately transferred to the OPV vacuum system for addition of C_{60} and BCP layers, deposited via sublimation at a base pressure at or below 8×10^{-7} torr.[38] A 10 MHz quartz crystal microbalance and a frequency counter (HP 5384A) were used to monitor deposition rate. All organic sublimation sources were prebaked at ~70% of the respective sublimation temperature for 30 min prior to film deposition to remove impurities. e-P3HT/ITO substrates were held in a separate vacuum chamber during prebaking of these sources to avoid surface contamination. A thickness of 40 nm C_{60} and 5 nm BCP were used for all PV devices, deposited at the respective rates of 1−2 Å/s and 2−10 Å/s. A vacuum deposited 100 nm thick Al cathode deposited at a rate of 1−2 Å/s was used as the top electrode. Aluminum deposition was monitored using a 6 MHz quartz crystal microbalance and an Inficon Deposition Monitor. Masks were placed over the deposited organic layers under nitrogen prior to aluminum deposition to create several circular devices on each e-P3HT film with a final area of 0.0288 cm^2. This configuration therefore provided several OPV devices from each electrodeposition experiment so that a statistically meaningful number of devices could be characterized with each electrodeposition procedure.

The completed OPV devices were returned to a N_2 atmosphere glovebox (model HE 493/MO-5, less than 1 ppm O_2 and H_2O) after aluminum deposition, without exposure to atmosphere. Multiple contacts were made to the ITO substrate, keeping the distance between these contacts and the center of each device less than 1 cm. Electrical contact to the aluminum top electrode was made using a gold wire gently pressed against this contact. Current−voltage measurements were made with a Keithley 2400 Source Meter, and data was recorded by Labview 5.1 (National Instruments). Scans were performed from 1.5 to −1.0 V with a step size of 10 or 20 mV. A CUDA Products Corp. fiber optic light source with a 250 W quartz halogen lamp (model I-250) was used as a light source (without the fiber optic). The light was filtered with diffuse and IR filters in order to limit heating of the OPVs. The light intensity at the OPV device was controlled by varying the distance between the light source and the device, with the power output of the light source monitored with a calibrated photodiode.

AFM Characterization. Atomic force microscopy was performed using a Dimension 3100 (Nanoscope, Digital Instruments, Santa Barbara, CA). Images were collected in tapping mode using ultrasharp cantilevers with a probe radius of curvature < 10 nm, a resonance frequency of 265−400 kHz, and a spring constant of 20−75 N/m (NSC15/AIBS MikroMasch, Wilsonville, OR). Images were obtained in air at scan rates of 0.5−1.0 Hz. The morphology and root-mean-square (rms) roughness were obtained from height images.

SEM Characterization. Scanning electrochemical microscopy was performed using a Hitachi S-3500 field emission SEM (FE-SEM) at 15 kV accelerating voltage at 100 000 magnification. Prior to image collection, samples were first coated in a thin (1−5 nm) layer of Pt.

Uv−Vis Spectroscopy. Spectroelectrochemical measurements were taken in the same electrochemical cell described above, mounted in the single beam path of an Agilent UV−vis spectrometer (no. 8453A, Foster City, CA) from 190 to 1100 nm. Spectra were collected with ChemStation software.

XPS Characterization of e-P3HT Films. XPS studies were performed with a Kratos Axis Ultra X-ray photoelectron spectrometer with a monochromatic Al Kα source at 1486.6 eV. For the data presented here, the analyzer had a pass energy of 20 eV. The XPS data was curve fit using Kratos software, peak fit with Gaussian peaks. A linear background subtraction was employed.

Photocurrent Action Spectra. Photocurrent action spectra were obtained using a Xenon arc source (Newport Oriel Instruments, Irvine, CA) and a Jobin Yvon monochromator (H10/1200, J-Y Optical Systems, Edison, NJ), with current monitored by a CH Instruments potentiostat (CHI 660, Austin, TX). Three current measurements were averaged for every 10 nm increment. Calibrations were obtained by monitoring the power output of the light source with respect to wavelength using a Newport Power Meter (1930 C, Newport Oriel Instruments, Irvine, CA). For wavelengths above 650 nm, a long pass filter was used (CVI Laser, Albuquerque, NM).

Results and Discussion

Potential Step Electrodeposition Protocols for e-P3HT Thin Films: AFM and SEM Studies of Electrodeposited Films. Prior to any electrochemistry, the indium tin oxide (ITO) substrates were first activated by brief exposures to

(37) Shallcross, R. C.; D'Ambruoso, G. D.; Korth, B. D.; Hall, H. K.; Zheng, Z. P.; Pyun, J.; Armstrong, N. R. *J. Am. Chem. Soc.* **2007**, *129*, 11310+.
(38) Brumbach, M.; Veneman, P. A.; Marrikar, F. S.; Schulmeyer, T.; Simmonds, A.; Xia, W.; Lee, P.; Armstrong, N. R. *Langmuir* **2007**, *23*, 11089–11099.
(39) Marrikar, F. S.; Brumbach, M.; Evans, D. H.; Lebron-Paler, A.; Pemberton, J. E.; Wysocki, R. J.; Armstrong, N. R. *Langmuir* **2007**, *23*, 1530–1542.

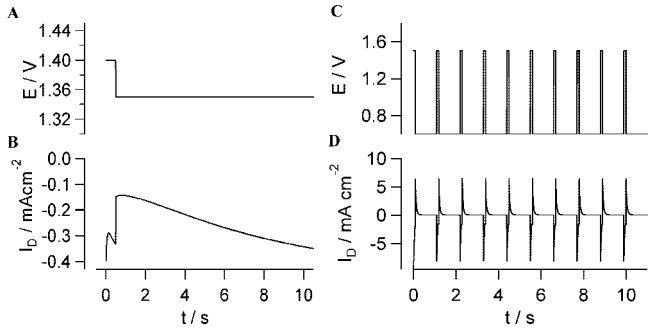

Figure 1. (A) Potential-time and (B) current−time profiles for electrodeposition of the e-P3HT carpet layer on HI-activated, 3-TAA modified ITO electrodes. (C) Potential−time and (D) current−time profiles for the electrodeposition/texturing steps for e-P3HT films; $V_{pulse} = +1.5$ V and $V_{rest} = +0.6$ V for 10 cycles.

concentrated HI,[38,39] followed by surface modification with a small molecule thiophene derivative, 3-thiophene acetic acid (3-TAA). This pretreatment has been previously reported by our group to enhance the rates of electron transfer to solution probe molecules[40,41] and appears to enhance rates of poly(thiophene) deposition by increasing the rate of oligomer/polymer nucleation during three-dimensional electrochemical growth.

Figure 1 shows the potential−time and current−time transients for the deposition of e-P3HT "carpet layer" thin films on 3-TAA modified ITO electrodes. Electrochemical deposition of P3HT films for the formation of the carpet layer was accomplished using a multipotential step profile developed specifically for the 3-TAA modified ITO electrode/e-P3HT system. The adsorbed 3-TAA monolayer has a slightly higher oxidation onset potential (ca. +1.4 V) versus the 3-hexylthiophene solution monomer (ca. +1.3 V); hence, we chose to use a two-step chronoamperometry sequence for film deposition (see Supporting Information section). The ITO electrode was initially stepped to 1.4 V for 0.5 s to initiate oxidation of the 3-TAA seed layer. The ITO electrode was then set to 1.35 V for 10−25 s, depending on desired e-P3HT film thickness. The initial large negative current in the first potential step is associated with double layer charging of the electrode and is followed by faradic current associated with oxidation of the 3-TAA monolayer. Upon decrease of the potential to 1.35 V, the faradic current from the deposition of e-P3HT increases and eventually reaches steady state (not shown), analogous to three-dimensional nucleation and growth of electrodeposited films.[42−44]

As shown in Figures 2A,B and 3A, the described electrodeposition process creates an e-P3HT film of approximately 15 nm thickness, with an rms roughness of less than approximately 2 nm. The AFM phase contrast image, which tends to be most sensitive to differences in crystallinity of polymer films, shows excellent uniformity of these carpet layer films over most of a 0.76 cm^2 film area. Both the AFM height images and the SEM data, viewed at higher magnification, suggest a subgrain structure to these films, with an average grain diameter of approximately 20 nm.

After formation of the carpet layer, the PPS electrodeposition protocol was used to increase the surface texture of these e-P3HT films (Figure 1C,D), with deposition parameters chosen to control three-dimensional nucleation and growth of the polymer film. It has been argued that electrodeposition of conductive polymers like poly(thiophenes) proceeds first through the formation oligomer thiophene chains in the solution phase adjacent to the electrode surface as a result of an electrocatalytic oxidation process.[45] Once these oligomer chains have grown to a sufficient molecular weight they precipitate onto the surface to form microclusters (nucleation). These clusters are believed to become thermodynamically stable upon reaching a critical size and begin to grow by incorporation of further oligomer species.[25]

The PPS protocol textures the e-P3HT film by termination of film growth after a brief nucleation event. During V_{pulse} (e.g., +1.5 V), e-P3HT film deposition occurs and the measured current results from both double layer charging and mass-transport controlled faradic current (Figure 1C,D). When the electrode is stepped to V_{rest} (e.g., +0.6 V), no polymer growth occurs and only double layer charging current is observed (enlarged view, Supporting Information), giving the thiophene monomer time to diffuse back to the film/liquid interface, "refilling" the original diffusion layer region.

A degree of morphological control is obtained using the PPS deposition technique. Since three-dimensional polymer growth is not restricted to the substrate plane, nucleation and growth rates are dependent upon applied potential and rates of mass transport.[46] In the PPS protocol, the pulses to overpotentials for monomer oxidation (V_{pulse}) are short enough to terminate growth after the nucleation step, promoting aggregate-like heterogeneous precipitation of oligomers onto the substrate. The long rest periods (V_{rest}), at potentials where no new polymer is formed, allows for thiophene monomer concentration at the polymer/solution interface to rebuild, via diffusion.[23] If the times for both deposition and rest potentials are similar and short relative to the time needed to refill the diffusion layer of monomer ($t \approx \delta^2/2D$; δ is the diffusion layer thickness, and D is the diffusion coefficient of the thiophene monomer (ca. 10^{-5} cm^2/s)[47]), the resultant e-P3HT films are roughened in the near surface region (Figures 2C,D and 3B). The AFM data suggests that the sizes of the individual nuclei depend on the rest potential time, with average diameters of the biggest features of approximately 150−300 nm for rest periods of 1 s. The SEM data shows grain-like texturing in the 50−100 nm range, with a subgrain structure showing features of approximately 5−20 nm in diameter. Variation in deposition and rest pulse times led to some variability in the texturing

(40) Carter, C.; Brumbach, M.; Donley, C.; Hreha, R. D.; Marder, S. R.; Domercq, B.; Yoo, S.; Kippelen, B.; Armstrong, N. R. *J. Phys. Chem. B* **2006**, *110*, 25191–25202.
(41) Donley, C.; Dunphy, D.; Paine, D.; Carter, C.; Nebesny, K.; Lee, P.; Alloway, D.; Armstrong, N. R. *Langmuir* **2002**, *18*, 450–457.
(42) Asavapiriyanont, S.; Chandler, G. K.; Gunawardena, G. A.; Pletcher, D. *J. Electroanal. Chem.* **1984**, *177*, 229–244.
(43) Genies, E. M.; Bidan, G.; Diaz, A. F. *J. Electroanal. Chem.* **1983**, *149*, 101–113.
(44) Li, F. B.; Albery, W. J. *Adv. Mater.* **1992**, *4*, 673–675.
(45) Heinze, J.; Rasche, A.; Pagels, M.; Geschke, B. *J. Phys. Chem. B* **2007**, *111*, 989–997.
(46) Bosco, E.; Rangarajan, S. K. *J. Electroanal. Chem.* **1982**, *134*, 213–224.
(47) Bard, A. J.; Faulkner, L. R. *Electrochemical methods - fundamentals and applications*, 2nd ed.; John Wiley & Sons, Inc.: New York, 2001.

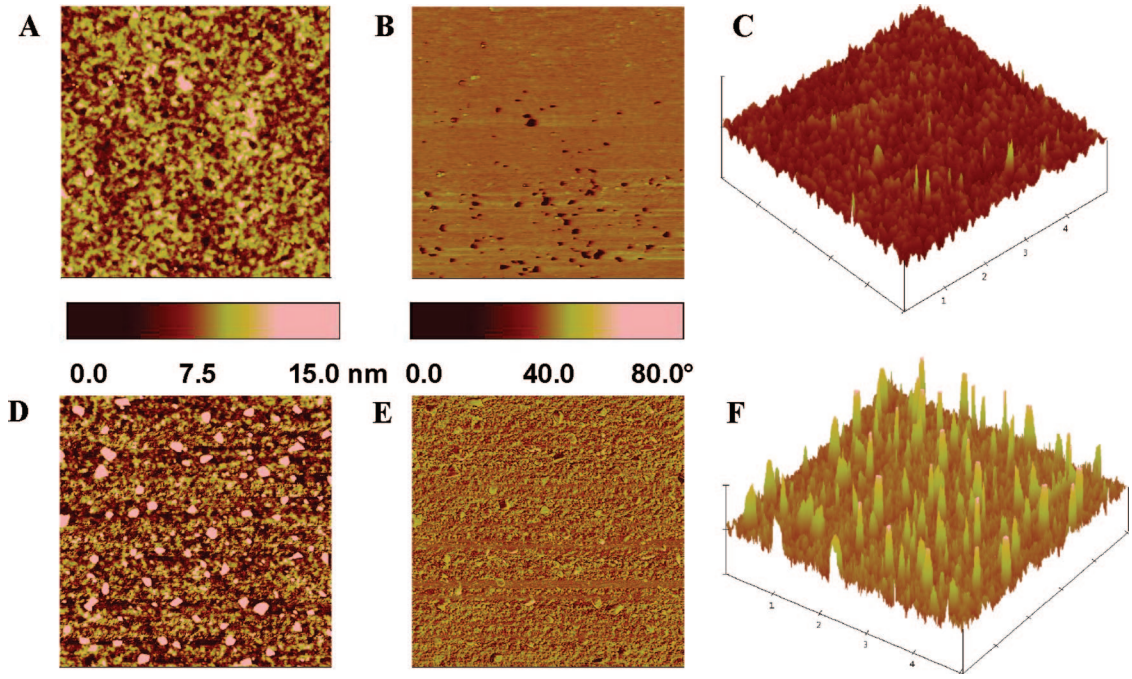

Figure 2. Tapping mode AFM images ($5 \times 5\ \mu m^2$) of e-P3HT films (A−C) "carpet layer" and (D−F) textured P3HT films created with the PPS protocols. (A, C, D, and F) are height images ($z = 0-15$ nm) and (B, D) are phase images ($z = 0-80.0°$).

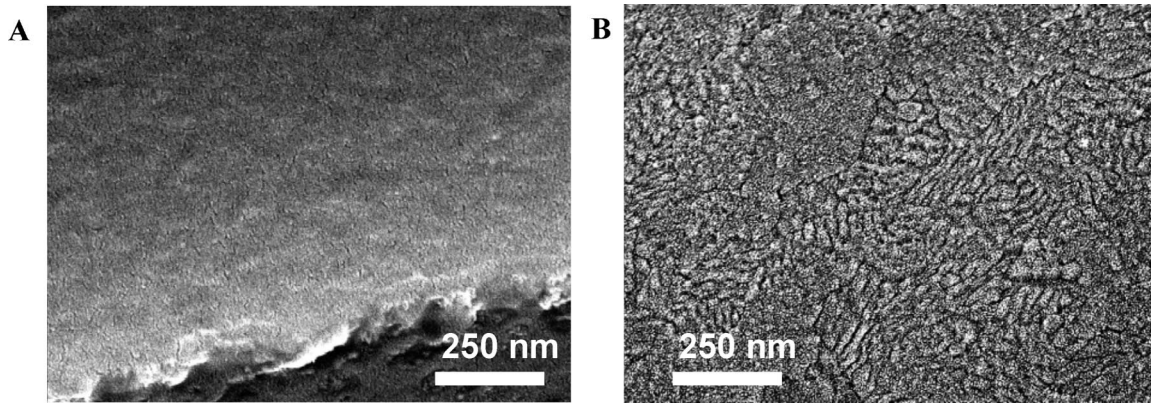

Figure 3. Field-emission SEM images of 1−5 nm Pt coated (A) e-P3HT carpet layer and (B) textured e-P3HT layers. Images were obtained with the samples tilted at a 45° angle. The image in (A) was obtained near an intentional break in the sample so that the polymer film profile down to the ITO substrate could be imaged.

of these films (see Supporting Information), but as shown below, the protocols summarized here generally led to the most electrically active films in PV device platforms (see below).

Characterization of e-P3HT Thin Films Using Voltammetry and Spectroelectrochemistry. Cyclic voltammetry was used to first estimate the surface coverage of the deposited polymer (Figure 4). Voltammetric sweeps were conducted from the fully reduced state of each film, to its fully oxidized (doped) state, and back. These voltammetric sweeps reveal several oxidation and reduction features, which were integrated together to coulometrically estimate relative surface coverages of each film. Texturing of e-P3HT films increased this coulometrically determined surface coverage by approximately 15% for each film (from voltammetric data), consistent with the above AFM and SEM data. AFM and SEM results indicate texturing of the outer surface region of these films but relatively small changes in film density.

Cyclic voltammetry and optical spectral data were also used to estimate the degree of regioregularity and conjugation length, as both the potentials for oxidation of the P3HT film and the absorbance spectra which result during oxidation/reduction vary depending on the degree of regioregularity and/or conjugation length.[48] In Figure 4A, cyclic voltammograms for both the carpet and textured e-P3HT films have unique current responses relative to spin cast P3HT (s-P3HT) films. For the s-P3HT films, which have a high degree of head-to-tail (HT) coupling/regioregularity, up to three voltammetric oxidation peaks are discernible at low voltammetric sweep rates (~0.64, ~0.82, and 0.95 V), indicative of three unique crystalline regions within the film. These peaks have been attributed to the presence of varying degrees of conjugation lengths within the film, with the shortest conjugation lengths doped at the highest oxidation

(48) Skompska, M.; Szkurlat, A. *Electrochim. Acta* **2001**, *46*, 4007–4015.

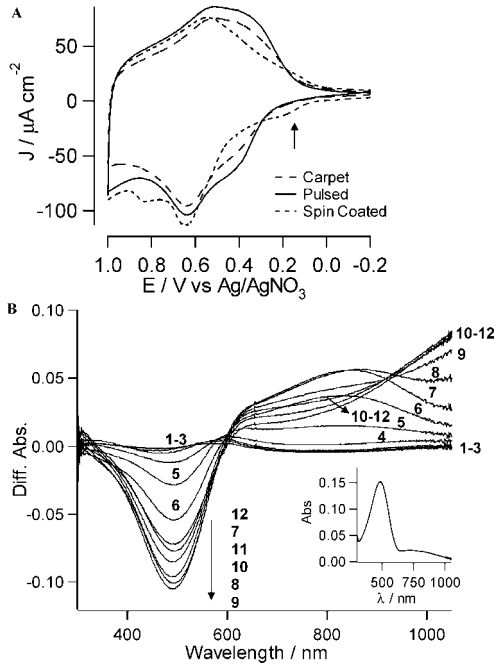

Figure 4. (A) Cyclic voltammograms of a spin coated P3HT film (ca. 20 nm thickness) (short dashed line) and two different e-P3HT films on ITO substrate, (long dashed line) carpet layer and (solid line) PPS textured layer. (B) UV/vis absorbance difference spectra of an e-P3HT (~20 nm, PPS textured) as the potential is stepped to (1) −0.1 V, (2) 0.0 V, (3) 0.1. V, (4) 0.2 V, (5) 0.3 V, (6) 0.4 V, (7) 0.5 V, (8) 0.6 V, (9) 0.7 V, (10) 0.8 V, (11) 0.9 V, and (12) 1.0 V. Spectra have been normalized by subtracting the absorbance at −0.2 V (inset).

potentials.[48−53] Films with lesser ordering and/or low regioregularity may show two or only one oxidation/reduction process, missing the highest oxidation potential peaks which are attributed to the thiophene segments with the shortest conjugation lengths.[48−51,54−56] Furthermore, for s-P3HT films, oxidation of the film begins at approximately +0.2 V (arrow), due to the higher concentration of HT couplings in this domain.[48,50,57]

The cyclic voltammogram for the carpet layer e-P3HT film (long dashed line) shows a more positive onset for oxidation of the polymer at approximately +0.4 V, and only a single broad redox wave is visible, with maximum current near 0.6 V. The cyclic voltammetry behavior of the carpet layer P3HT films is indicative of films with little regioregularity and random coupling, which are mostly noncrystalline.[48,51] Electrodeposition methods have previously provided poly(alklythiophene) films with regioregularity less than 70%[58] but with a high degree of structural order and extended

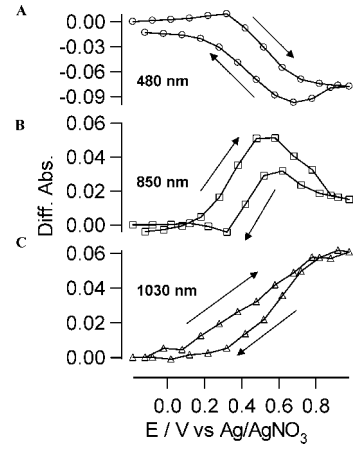

Figure 5. Differential absorbance versus potential for an e-P3HT film (textured), at wavelengths corresponding to the absorbance of the (A) neutral, undoped form (480 nm), (B) the polaronic (one-electron oxidation) state (850 nm), and (C) the absorbance of the a multipolaron state (1030 nm).

π-conjugation lengths.[48,49,57] In addition to the increased current due to added polymer, the cyclic voltammogram for the textured e-P3HT film (solid line) shows a unique feature, with the presence of two oxidation/reduction peaks. The major contribution to increased oxidative current arises from the enhanced shoulder to the main oxidation peak at approximately +0.4 V, preceding the prominent oxidation peak at +0.6 V. This extra shoulder peak near +0.4 V has not been previously reported and is indicative of the formation of new polymer domains that are more easily oxidized/reduced than the domains associated with the voltammetric peak near 0.6 V, resulting from the enhanced roughness of the e-P3HT film after the PPS deposition protocols. This redox process is reversible over repeated voltammetric scans; that is, no electrochemical degradation occurs upon cycling or doping as the film is transitioned between the polaronic and bipolaronic (neutral and oxidized) states.

The UV/vis absorption spectra for the textured P3HT films are shown in Figures 4B and 5. In both figures, the absorbance spectra are presented with respect to applied potential and have been normalized by subtracting the absorbance spectrum at −0.2 V (neutral state) from each data set. Figure 4B gives the entire absorbance spectrum with respect to doping potential; Figure 5 tracks the change in absorbance at 480, 850, and 1030 nm with respect to applied potential. The inset in Figure 4B shows the raw absorbance spectrum for the neutral state at −0.2 V.

In Figures 4B and 5, there is evidence of three distinct redox states in e-P3HT films, illustrated by the two isosbestic points at ~630 and ~940 nm, suggestive of a two step oxidative doping process. The neutral state has a maximum absorbance near 480 nm,[48,52] attributed to the main $\pi-\pi^*$ transition, which decreases as the film transitions from the neutral to the oxidized state.[52] At moderate doping potentials between 0.4 and 0.8 V, the polaronic state is formed and has a maximum near 850 nm (Figure 5B). Progression to doping potentials above 0.8 V shows evidence of the multipolaronic states of P3HT, indicated by the unique line shape from 800−1100 nm (Figure 5C). The multipolaronic state has previously been reported as the transition from

(49) Skompska, M. *Electrochim. Acta* **1998**, *44*, 357–362.
(50) Skompska, M.; Szkurlat, A.; Kowal, A.; Szklarczyk, M. *Langmuir* **2003**, *19*, 2318–2324.
(51) Trznadel, M.; Zagorska, M.; Lapkowski, M.; Louarn, G.; Lefrant, S.; Pron, A. *J. Chem. Soc., Faraday Trans.* **1996**, *92*, 1387–1393.
(52) Trznadel, M.; Pron, A.; Zagorska, M. *Macromolecules* **1998**, *31*, 5051–5058.
(53) Trznadel, M.; Pron, A.; Zagorska, M. *Synth. Met.* **1999**, *101*, 118–119.
(54) Chen, X. W.; Inganas, O. *J. Phys. Chem.* **1996**, *100*, 15202–15206.
(55) Sato, M.; Tanaka, S.; Kaeriyama, K. *Makromol. Chem. - Macromol. Chem. Phys.* **1987**, *188*, 1763–1771.
(56) Li, Y. F.; Qian, R. Y. *J. Electroanal. Chem.* **1993**, *362*, 267–272.
(57) Skompska, M. *Electrochim. Acta* **2000**, *45*, 3841–3850.
(58) Leclerc, M.; Diaz, F. M.; Wegner, G. *Makromol. Chem. - Macromol. Chem. Phys.* **1989**, *190*, 3105–3116.

Scheme 1. Neutral and Doped States of P3HT

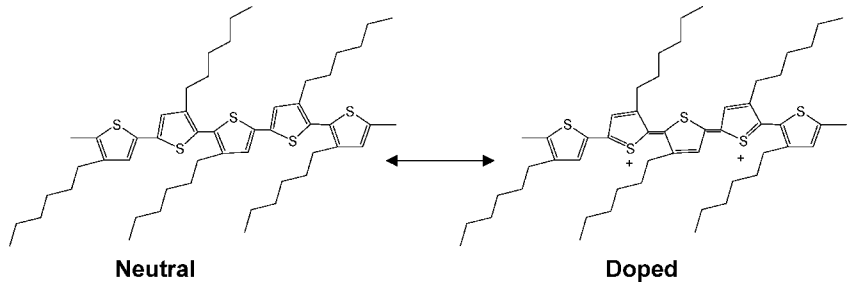

upper bipolaron to a quasi-metallic behavior in regioregular films[48,59,60] and has previously been demonstrated to have the highest degree of conductivity.[61]

These extremely thin e-P3HT films yield unexpected behavior at high doping potentials, with the return of some of the absorbance intensity at 480 nm (Figure 5A), suggesting disproportionation of redox states in close proximity and a reintroduction of the neutral state. The increase in absorbance at 480 nm (neutral state) at high applied potentials (>0.8 V) coincides with a loss in the absorbance of the polaronic state at 850 nm (Figure 5B) and minimal change in absorbance for the mulit-polaronic state at 1030 nm (Figure 5C). Analogous behavior to that described above has been seen before in conductive polymers in different electrolytes.[26] The spectroelectrochemical data suggest a unique equilibrium between neutral, photoactive domains and doped, conductive domains, upon moderate to high levels of electrochemical doping. The precise location and degree of segregation between neutral and doped domains with respect to electrochemical technique remains unclear.

Characterization of Neutral and Oxidized (Doped) e-P3HT Films Using X-ray Photoelectron Spectroscopy. XPS was used to quantify the degree of doping, monitor the incorporation of the electrolyte, and probe the relative percentage of dopant domains within the P3HT film, as described by the spectroelectrochemical data. XPS was conducted on both carpet and textured e-P3HT films as a function of electrochemical doping conditions, at both normal and high photoemission takeoff angles (60°), to estimate the degree of homogeneity in the doping process shown in Scheme 1.

The experimental data and fits for photoemission at high takeoff angles (60°) are given in Figure 6 and Table 1, with the model used to fit the data and the corresponding binding energies and relative fitted peak area percentages presented in Supporting Information. The energy values and peak areas for the F(1s) peak arising from the incorporation of the anion of the electrolyte (PF_6^-) during the oxidative doping process are also give in Table 1. The degree of oxidation reported throughout the text is given as the average of the S(2p) and

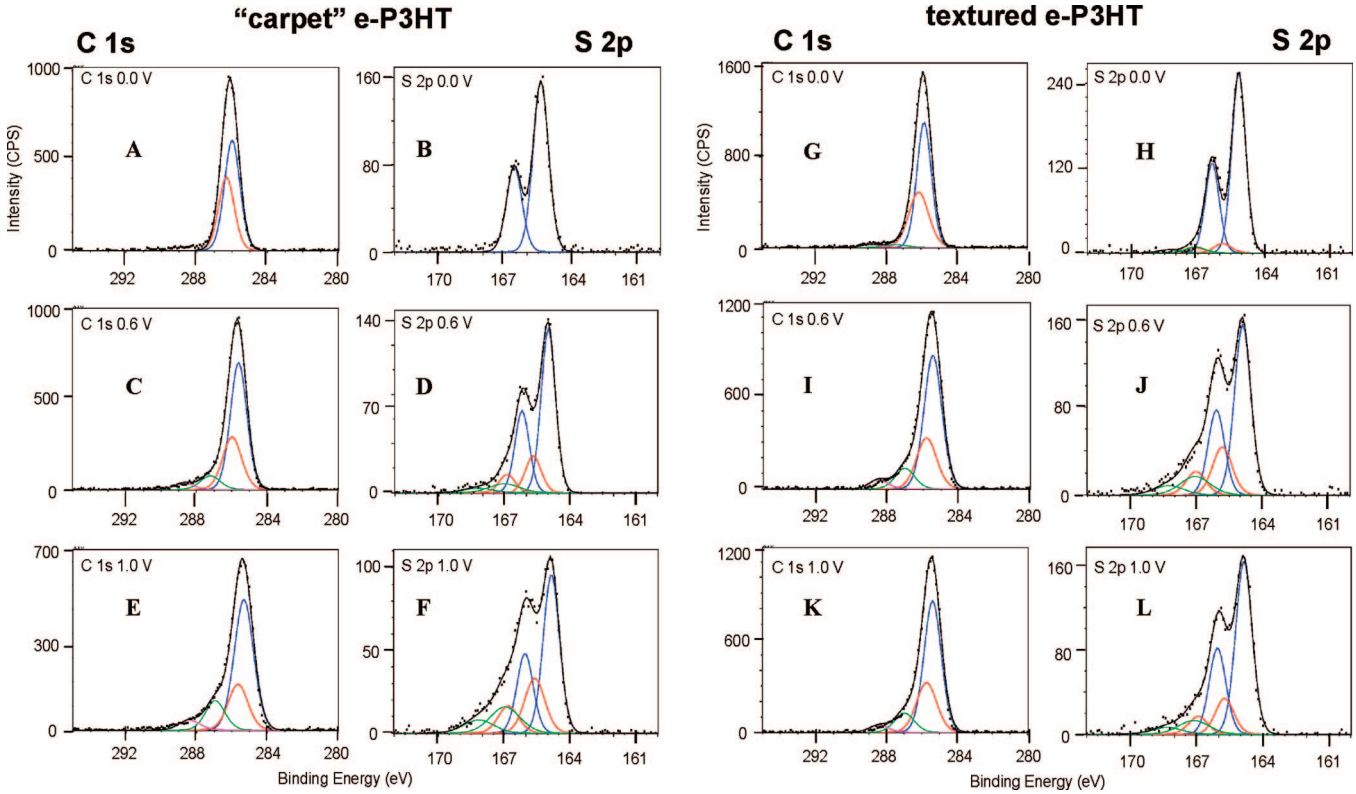

Figure 6. (A−L) C(1s) and S(2p) XPS data (60° takeoff angle) for "carpet" layer e-P3HT films (A−F) and textured e-P3HT films (G−L). Fitting parameters for both the C(1s) and S(2p) data described in text and in Supporting Information.

Table 1. Quantitation of XPS Data for Electrochemically Doped e-P3HT Films for "Carpet" and Textured e-P3HT Films at 0° and 60° Takeoff Angles

	0.0 V doping potential		0.6 V doping potential		1.0 V doping potential	
	0°	60°	0°	60°	0°	60°
Carpet e-P3HT Films						
sulfur from oxidized thiophene units[a]			22.7%	26.7%	35.4%	42.4%
carbon from oxidized thiophene units[b]			25.9%	28.6%	42.0%	46.5%
F/S atomic ratio[c]			0.906	0.493	1.077	0.926
F/C atomic ratio[c]			0.561	0.407	1.443	0.866
degree of oxidation[d]			24.3%	27.7%	38.7%	44.4%
Textured e-P3HT Films						
sulfur from oxidized thiophene units[a]	9.7%	9.8%	34.2%	34.8%	30.9%	27.3%
carbon from oxidized thiophene units[b]	10.0%	9.5%	34.6%	35.8%	38.1%	34.1%
F/S atomic ratio[c]	0.093	0.114	0.742	0.623	0.725	0.577
F/C atomic ratio[c]	0.064	0.074	0.523	0.434	0.487	0.395
degree of oxidation[d]	9.8%	9.7%	34.4%	35.3%	34.5%	30.7%

[a] Data obtained from fitting of the S(2p) spectral region.[39,62,72] [b] Data obtained from fitting of the C(1s) spectral region (thiophene ring carbons only).[62,72] [c] Fluorine entrapped in the e-P3HT film after electrochemical doping, from PF_6^-. [d] Degree of oxidation is calculated by averaging the percent doping for the respective S(2p) and C(1s) peaks.

C(1s) doping percentages given in Table 1. The degrees of doping with respect to electrochemical potential for both carpet and pulsed films at high takeoff angles are discussed below.

The initial fits for both the C(1s) and S(2p) peaks were derived from best fits for the fully reduced carpet layer (Figure 6A,B). The C(1s) spectra for the fully reduced carpet e-P3HT films in Figure 6A are described by a two component fit, consistent with the assignment of two forms of carbon in the polymer, those of the alkyl side chains (BE = ~286 eV) and those arising from the aromatic ring (BE ~ 286.4 eV). The two carbon types were optimized to an energy separation of 0.331 eV and an atomic ratio of 3:2, as dictated by the chemical structure. Previous XPS characterization of undoped poly(thiophene) films have found a C(1s) splitting of 0.34 ± 0.12 eV;[62] no data to date has been reported for doped poly(thiophenes). The S(2p) region was fit with a single $S(2p_{1/2,3/2})$ doublet, maintaining a ratio of 2:1 and a peak energy separation of 1.203 eV (Figure 6B), consistent with previously reported results of 1.25 eV for thiophene.[62]

For doped versions of both the carpet and textured e-P3HT films, the C(1s) and S(2p) spectral envelopes showed evidence for additional oxidized (polaron) thiophene forms, with the effect being most pronounced in the S(2p) spectra (Table 1 and Supporting Information Tables 1 and 2). Two additional S(2p) doublets were added to fit the spectral envelopes, under the assumption of the creation of two additional states from the spectroelectrochemical data, with BE shifts of 0.9 and 2.1 eV for the two additional sets of peaks. Previous XPS data for electrochemically doped poly(3,4ethylenedioxythiophene), or PEDOT, has been fit using two additional S(2p) doublets to describe the XPS data for doped states of the PEDOT films.[39,63] To correlate with the S(2p) data, two additional C(1s) ring components were used to fit the carbon XPS data, at energy separations of 1.255 and 2.726 eV from the neutral aromatic ring carbon.

In Table 1, the degrees of oxidation for the textured and carpet e-P3HT films are compared with respect to doping potential at high and normal takeoff angle XPS. At 0.0 V, while the carpet film showed no oxidation, there is a slight oxidation found in the textured e-P3HT film as well as the presence of a small F(1s) peak. This suggests that electrolyte has been trapped within the film with each growth cycle and a small amount of doping is sustained when the film is immersed.

For doping at 0.6 V, the degree of oxidation (average for S(2p) and C(1s)) for the textured versus the carpet e-P3HT layers was slightly higher (35% versus ~28% of the thiophene rings appeared to be oxidized). For normal takeoff angles, the degree of doping of thiophene was approximately 34%:24% (textured/carpet), suggesting considerable uniformity with depth in the doping process. For the textured e-P3HT films, F(1s):S(2p) or F(1s):C(1s) area ratios were similar in both the high and the normal takeoff angle spectra (Table 1). For the carpet e-P3HT films, however, significantly higher F(1s):S(2p) or F(1s):C(1s) ratios were observed for normal takeoff angle XPS data, versus the high takeoff angle, suggesting that electrolyte is more concentrated below the surface of the film when using chronoamperometry to dope the film.

For films doped at potentials of 1.0 V, there are significant differences between the carpet and textured films. The carpet layer shows an increased level of doping at both high (44%) and normal (39%) takeoff angles, again, with higher F(1s) area ratios for normal takeoff angles (>1). However, the textured film shows only a slight decrease in doping for both normal (34%) and high (31%) takeoff angles, and slightly lower F(1s) area ratios, relative to films doped at +0.6 V.

(59) Sato, M.; Tanaka, S.; Kaeriyama, K. *Synth. Met.* **1986**, *14*, 279–288.
(60) Chung, T. C.; Kaufman, J. H.; Heeger, A. J.; Wudl, F. *Phys. Rev. B* **1984**, *30*, 702–710.
(61) Jiang, X.; Harima, Y.; Yamashita, K.; Tada, Y.; Ohshita, J.; Kunai, A. *Chem. Phys. Lett.* **2002**, *364*, 616–620.
(62) Gelius, U.; Allan, C. J.; Johansso, G.; Siegbahn, H.; Allison, D. A.; Siegbahn, K. *Phys. Scr.* **1971**, *3*, 237-&
(63) Crispin, X.; Marciniak, S.; Osikowicz, W.; Zotti, G.; Van der Gon, A. W. D.; Louwet, F.; Fahlman, M.; Groenendaal, L.; De Schryver, F.; Salaneck, W. R. *J. Polym. Sci., Part B: Polym. Phys.* **2003**, *41*, 2561–2583.

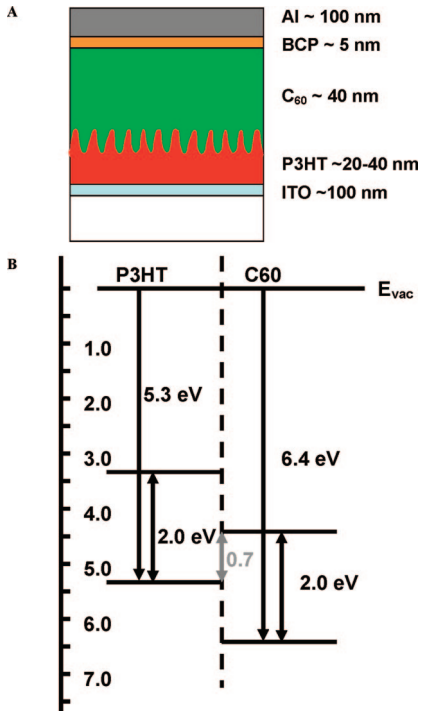

Figure 7. (A) Schematic of the "planar heterojunction" e-P3HT/C_{60} OPV, showing the anticipated extent of mixing of the two layers; (B) energy level offsets for P3HT relative to C_{60} (no correction for the probable interface dipole shifts upon doping at the P3HT/C_{60} interface).

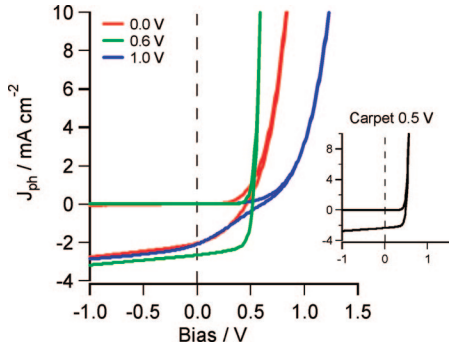

Figure 8. *J*/*V* curves for dark and illuminated (100 mW/cm^2 white light source) for textured e-P3HT layers, emmersed at doping potentials of 0.0 V (red), 0.6 V (green), and 1.0 V (blue). The *J*/*V* response for a "carpet" e-P3HT film, doped to a potential of 0.5 V, is shown in the inset.

This small decrease in doping may be indicative of the disproportionation suggested by the spectroelectrochemical data; however, we have previously noted loss of oxidative doping of organic films created above certain potentials during transfer to an ex situ technique such as XPS.[64] It is difficult to emmerse overoxidized polymer films from electrolyte solutions without some loss of oxidative doping in the process. Further work is necessary to fully characterize this phenomenon.

Characterization of Planar Heterojunction Photovoltaic Activity of e-P3HT Films Using C_{60} as the Electron Acceptor Layer. Photovoltaic devices were created for both carpet and textured e-P3HT films (Figures 7 and 8) in their undoped states (red line, 0.0 V) and for films doped at potentials of 0.6 (green line) and 1.0 V (blue line). These *J*/*V* curves are representative of at least five devices from each film type (up to 12 devices could be made and tested on each electrodeposited film, see Experimental Section). Once formed electrochemically, these e-P3HT films were rinsed in dry solvent, transferred to a nitrogen atmosphere, and then introduced to the high vacuum deposition chamber. Planar heterojunction-like OPVs were created by sequential deposition of C_{60}, BCP, and aluminum (top electrode) layers onto the e-P3HT film.[33−36] A schematic of these devices and a suggested energy level diagram for the e-P3HT (neutral state)/C_{60} heterojunction is given in Figure 7 (based on data from refs 10, 47, and 65−68), with a predicted built-in potential V_{BI} of ~0.7 V based on the offsets between the HOMO of the P3HT layers and the LUMO of the C_{60} layer ($E_{HOMO;3\text{-}P3HT} - E_{LUMO;C60}$—derivation given in Supporting Information). Figure 8 gives representative dark and illuminated (100 mW/cm^2 white light) plots for each doped textured e-P3HT film and best performing carpet device, with data summarized in Table 2 and corresponding semilog plots given in the Supporting Information. No statistically significant changes in V_{OC} with respect to doping potential were observed, in contract to previous reports by Frohne et al. for electrochemical doping of PEDOT layers under photoactive bulk heterojunction OPVs.[69]

For all of the cells created, the degree of rectification in the dark was strongly dependent upon the final doping treatment, comparing currents at forward and reverse bias at ± 0.6 V, the rectification ratios were approximately 49, 2.6 × 10^4, and 141 for e-P3HT films, doped at 0.0, +0.6, and +1.0 V, respectively. Films doped to +0.6 V showed the highest rectification ratios, suggesting that leakage pathways and recombination centers were minimized in these films. Optimized PV performance was also obtained for textured e-P3HT films doped at 0.6 V prior to device fabrication, with an average series resistance, R_S, of less than 0.5 Ω·cm^2, a shunt resistance R_P greater than 1.6 × 10^5 Ω·cm^2, V_{OC} approximately 0.5 V, maximum J_{SC} values up to approximately 3 mA/cm^2, fill factors (FF) routinely near or above 0.65, and power conversion efficiencies consistently near 1%. Of note is that for e-P3HT films left in their neutral states, V_{OC} is comparable to doped films, but both J_{SC} and FF values were compromised, with significant impact on both R_S and R_P (Table 2). A similar effect was noted for e-P3HT films doped at 1.0 V, with a larger impact on FF and R_S. Figure 8 also compares the *J*/*V* data for the best e-P3HT carpet film (inset, doped to 0.5 V) and textured e-P3HT films doped to 0.6 V (green line), showing that the added texturing increases the J_{SC} by approximately 20%, consistent with the hypothesis that texturing creates increased surface area at the e-P3HT/C_{60} interface for improved exciton dissociation and charge formation (Figure 7). Solution deposition treatments with other electron acceptor fullerenes and semicon-

(64) Ferencz, A.; Armstrong, N. R.; Wegner, G. *Macromolecules* **1994**, *27*, 1517–1528.
(65) Micaroni, L.; Nart, F. C.; Hummelgen, I. A. *J. Solid State Electrochem.* **2002**, *7*, 55–59.
(66) Pavlishchuk, V. V.; Addison, A. W. *Inorg. Chim. Acta* **2000**, *298*, 97–102.
(67) Trasatti, S. *J. Electroanal. Chem.* **1983**, *150*, 1–15.
(68) Seo, J. H.; Kang, S. J.; Kim, C. Y.; Cho, S. W.; Yoo, K. H.; Whang, C. N. *Appl. Surf. Sci.* **2006**, *252*, 8015–8017.
(69) Frohne, H.; Shaheen, S. E.; Brabec, C. J.; Muller, D. C.; Sariciftci, N. S.; Meerholz, K. *ChemPhysChem* **2002**, *3*, 795+.

Table 2. Representative Data for Planar Heterojunction OPVs Based on e-P3HT

	type of e-P3HT film			
	textured e-P3HT 0.0 V	textured e-P3HT 1.0 V	textured e-P3HT 0.6 V	carpet (0.5 V)
J_{SC} (mA·cm^{-2})	−2.03	−2.05	−2.72	−2.31
V_{OC} (V)	0.47	0.56	0.50	0.50
FF	0.37	0.29	0.66	0.68
R_S (Ω·cm^2)	2.88	10.59	0.45	0.41
R_P (Ω·cm^2)	2513	38741	164430	256024
degree of rectification (±0.6 V)	49	141	26400	18700

ductor and oxide nanoparticles are underway, where the effect of increased surface area is anticipated to be even more significant.

Figure 9A,B shows J_{SC} and FF values for identical OPVs created from carpet (▲) and textured (■) e-P3HT films, as a function of final doping potential, with white light illumination at 100 mW/cm^2. For textured e-P3HT films, there is a clear maximum in J_{SC} and FF for OPVs created from e-P3HT emmersed at potentials of 0.6 V. Carpet e-P3HT films have low J_{SC} and FF values, and no clear trend with respect to doping potential is observed. Most significantly, while the increase in film thickness of textured film over the carpet films is quite small, the improved photocurrent appears to be a direct product of the doping technique. Specifically, it is believed that the PPS deposition technique creates and maintains, upon emmersion, isolated domains of neutral, photoactive regions and phase separated, electrically conductive, doped domains near the donor/acceptor interface. In theory, the domains are in close proximately to one another such that charges are generated at the interface of the neutral, photoactive region of the P3HT film and the fullerene but are readily transported away from the interface to the electrode by the doped, conductive P3HT domains. The XPS data suggested a pronounced dispersion of doped domains throughout the thickness of the film for the e-P3HT carpet films, doped by chronoamperometry. The net result seems to be an increase in recombination sites with this architecture, leading to a decrease in photocurrent. Further work is planned to fully probe the configuration of the P3HT films at the interface.

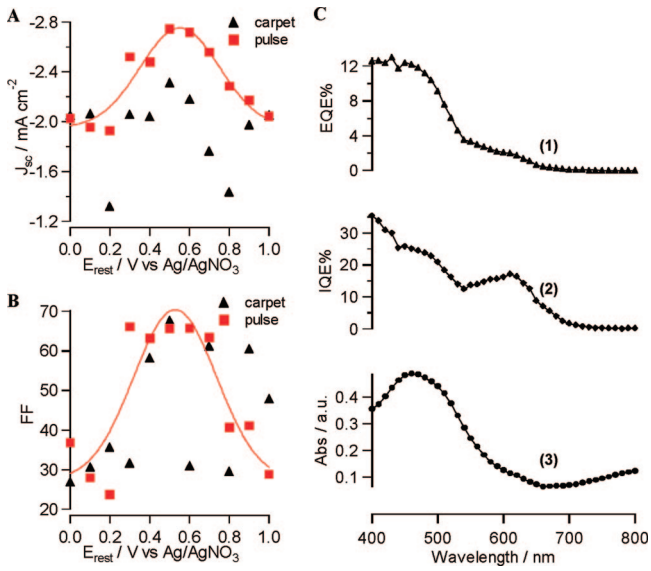

Figure 9. (A) J_{SC} versus doping potential for textured and carpet layer e-P3HT films in a e-P3HT/C_{60} heterojunction OPV; (B) fill factors (FF) as a function of doping potential for the same set of e-P3HT films. (C) Absorbance and photocurrent action spectra for an optimized e-P3HT/C_{60} heterojunction, where the textured e-P3HT was doped at 0.6 V as described above: (1) external (incident light) quantum efficiency; (2) internal quantum efficiency; and (3) absorbance spectrum.

Figure 9C shows the absorbance and photocurrent action spectra for an optimized OPV based on a textured e-P3HT/C_{60} heterojunction. The absorbance spectra are as expected for e-P3HT/C_{60} heterojunctions, without the low energy absorbance shoulders attributable to highly regioregular P3HT films.[48,59,60] Of interest are the EQE and particularly the IQE plots, which show high efficiencies in the 400 to 500 nm region and then decrease at wavelengths above 700 nm. There are spectral features in the IQE plot in the region from 600 to 700 nm, which is a region associated with the polaronic state of the thiophene polymer, which is not expected to contribute to photocurrent production. Further studies are underway to fully understand the unique behavior of textured e-P3HT films in photovoltaic applications.

Conclusions

We have summarized our initial steps toward the use of electrodeposition to both fabricate and texture polythiophenes and related donor polymers for energy conversion materials. Extremely thin films (20 nm) were used because the thickness is on the order of the exciton diffusion length and affects of doping and texturing are the most pronounced in this thickness regime. The V_{OC} values are consistent with expectation for P3HT/C_{60} heterojunctions and smaller than for the P3HT/PCBM heterojunctions, since C_{60} has an electron affinity approximately 0.1 eV higher than PCBM.[3,70,71] J_{SC} values seen to date are lower than seen in optimized P3HT/PCBM cells; however, our optimized P3HT films are substantially thinner than typical spin-cast P3HT/PCBM films. The IQE values for our optimized OPVs actually exceed IQE values for nonannealed P3HT/PCBM cells.[21] We have also seen a significant dependence of device performance on doping of the donor polymer e-P3HT layer. Optimally doped e-P3HT films lead to the most efficient photovoltaic devices thus far seen for electrodeposited donor layers, and it is clear that electrodeposition needs to be reexamined as an approach for the creation of OPV materials.

(70) Wudl, F. *Acc. Chem. Res.* **1992**, *25*, 157–161.
(71) Allemand, P. M.; Koch, A.; Wudl, F.; Rubin, Y.; Diederich, F.; Alvarez, M. M.; Anz, S. J.; Whetten, R. L. *J. Am. Chem. Soc.* **1991**, *113*, 1050–1051.
(72) Beamson, G.; Briggs, D. *High Resolution XPS of Organic Polymers: The Scienta ESCA300 Data Base*; John Wiley & Sons: New York, 1992.

Work in progress focuses on using electrodeposited polymer films as base layers for both photovoltaic and photoelectrochemical energy conversion devices, increasing the donor/acceptor interfacial surface area and increasing photocurrent through the inclusion of photoactive components, such as nanoparticles, or the implementation of a multijunction solar cell configuration.

Acknowledgment. This work was supported by a grant from the U.S. Department of Energy, DE-FG03-02ER15378, the National Science Foundation CHE 0517963, the NSF-Center for Materials and Devices for Information Technology, DMR-0120967, the Office of Naval Research, and the Arizona Board of Regents, TRIF fund for Arizona Research in Solar Energy (AzRISE).

Supporting Information Available: Linear sweep voltammetry, potential pulse protocol schematics, XPS model and data tables, derivation of the energy level diagram, and the semilog J/V curves for the dark and illuminated textured e-P3HT films (PDF). This material is available free of charge via the Internet at http://pubs.acs.org.

CM8008122